

Relating Airway Diameter Distributions to Regular Branching Asymmetry in the Lung

Arnab Majumdar,^{1,2} Adriano M. Alencar,² Sergey V. Buldyrev,^{1,3} Zoltán Hantos,⁴ Kenneth R. Lutchen,²
H. Eugene Stanley,¹ and Béla Suki²

¹Center for Polymer Studies and Department of Physics, Boston University, Boston, Massachusetts, 02215 USA

²Department of Biomedical Engineering, Boston University, Boston, Massachusetts, 02215 USA

³Department of Physics, Yeshiva University, New York, New York, 10033, USA

⁴Department of Medical Informatics and Engineering, and Institute of Surgical Research, University of Szeged, Hungary

(Received 1 March 2005; published 12 October 2005)

We study the distribution $\Pi_n(D)$ of airway diameters D as a function of generation N in asymmetric airway trees of mammalian lungs. We find that the airway bifurcations are self-similar in four species studied. Specifically, the ratios of diameters of the major and minor daughters to their parent are constants independent of N until a cutoff diameter is reached. We derive closed form expressions for $\Pi_N(D)$ and examine the flow resistance of the tree based on an asymmetric flow division model. Our findings suggest that the observed diameter heterogeneity is consistent with an underlying regular branching asymmetry.

DOI: 10.1103/PhysRevLett.95.168101

PACS numbers: 87.19.Rr, 87.19.Tt, 87.19.Uv, 87.80.Pa

Leonardo da Vinci observed five centuries ago that “all the branches of a tree at every stage of its height when put together are equal in thickness to the trunk” [1]. Similar regularities are seen in distribution networks of plants, and the respiratory and vascular systems in mammals [2]. The ubiquity of regular branching structures has led to the study of underlying optimization principles [3], as well as the development of growth models governed by local rules of branching [4]. The variation of size with generation is related to allometric scaling of metabolic rate with body mass [5].

Most models of the lung airway tree either do not address the observed diameter heterogeneity or simply consider it a result of random fluctuations. Here, we examine the branching pattern of the airway tree in mammalian lungs, and demonstrate that the simplifying assumption of deterministic branching asymmetry is sufficient to account for the observed distribution of airway diameters at any level of branching. In addition, we find that the same form of asymmetry can determine the resistance to air flow in the lung.

We first introduce some notation [6]. We label each airway in the tree by a pair of indices (i, j) , where the index i is the generation number of the airway and the index j ($0 \leq j < 2^i$) is used to distinguish between airways of the same generation. The root of the tree, the trachea, is labeled $(0, 0)$. The daughters of a bifurcating airway (i, j) are $(i + 1, 2j)$ and $(i + 1, 2j + 1)$ (Fig. 1).

The diameter of airway (i, j) relative to the diameter of the root is defined as $D_{i,j}$, with $D_{0,0} = 1$. The daughter with the smaller (larger) diameter is termed the *minor* (*major*) daughter and labeled by an even (odd) value of j . We define the diameter ratios κ_{\min} and κ_{\max} , respectively, as the ratios of diameters of the *minor* and *major* daughter to their parent (Fig. 1),

$$\kappa_{\min} \equiv D_{i+1,2j}/D_{i,j} \quad (1a)$$

$$\kappa_{\max} \equiv D_{i+1,2j+1}/D_{i,j}. \quad (1b)$$

We analyze the airway diameters from published data on four species: dog, rat, human, and rabbit [7,8]. Figure 2 shows the mean and standard deviations of κ_{\min} and κ_{\max} as functions of generation number N for one animal from each species. For all four species, we find that values of κ_{\min} and κ_{\max} are significantly different from each other and are independent of N . Table I shows the average values of κ_{\min} and κ_{\max} . Figure 3 shows an example of the diameter distribution $\Pi_N(D)$ and Fig. 4 shows mean airway diameters $\langle D_N \rangle$ and their standard deviations $\sigma(D_N)$ as functions of N .

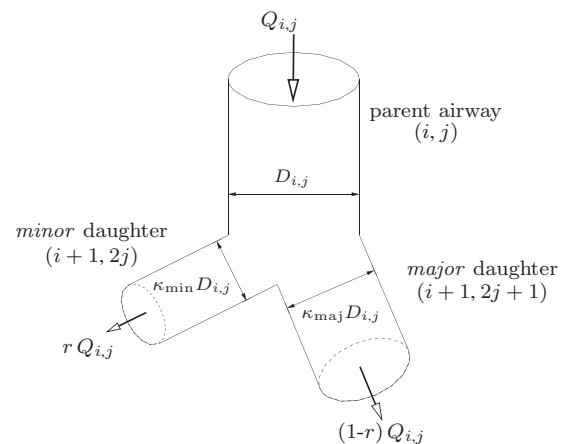


FIG. 1. Illustration of the notation and model. The *major* (*minor*) daughter corresponds to the daughter airways with larger (smaller) diameter. The diameter ratios κ_{\max} and κ_{\min} defined in Eq. (1) are constant at every bifurcation in the tree. The flow $Q_{i,j}$ of the parent airway (i, j) is partitioned according to Eq. (2).

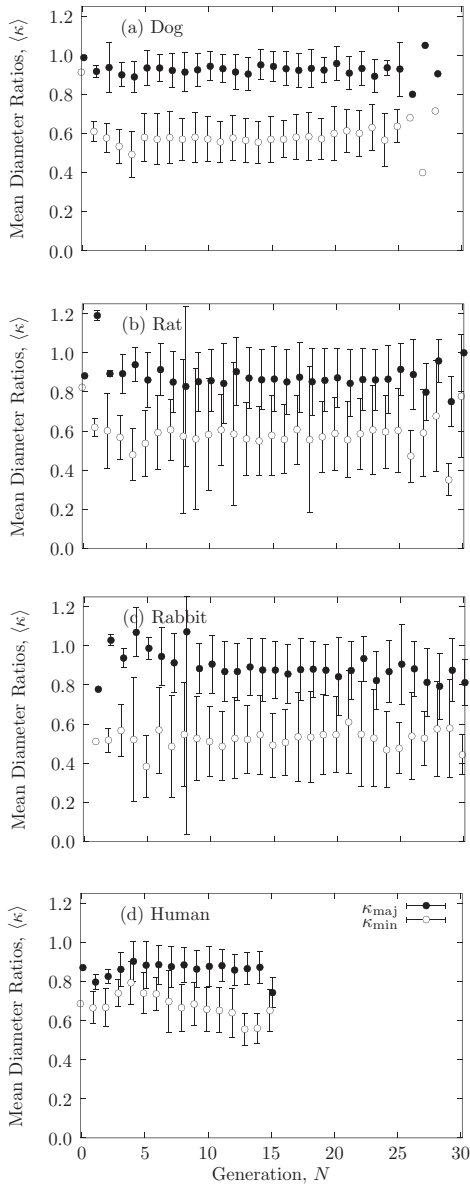


FIG. 2. Mean diameter ratios for the major (κ_{maj} , ●) and minor (κ_{min} , ○) daughters as a function of generation number N for one animal from each of four different species: (a) dog, (b) rat, (c) rabbit, and (d) human. The error bars show the standard deviation of the corresponding distributions at each N .

The flow $Q_{i,j}$ is defined for each airway (i, j) , with $Q_{0,0} = 1$. At each bifurcation, the flow $Q_{i,j}$ of a parent airway is partitioned between its daughters $Q_{i+1,2j}$ and $Q_{i+1,2j+1}$ according to

$$Q_{i+1,2j} = rQ_{i,j} \quad (2a)$$

$$Q_{i+1,2j+1} = (1-r)Q_{i,j} \quad (2b)$$

where the parameter $r \leq \frac{1}{2}$ determines the asymmetry of flow partitioning (Fig. 1). For simplicity, we assume the

same partitioning of air flow at each bifurcation, so r is a constant [4].

We assume that the dimensionless diameter $D_{i,j}$ of an airway (i, j) is related to the dimensionless flow $Q_{i,j}$ [9] as

$$Q_{i,j} = (D_{i,j})^\eta, \quad (3)$$

where the exponent η is the same for all generations within the airway tree. Equation (3) arises from the optimization of diameters of a single tube in order to minimize dissipation while maintaining biological viability. For laminar flow the optimum value of $\eta = 3$ [9], while for turbulent flow $\eta = 2.33$ [10]. The former result has also been extended for symmetric fractal trees [5].

We can express the diameter ratios by combining Eqs. (1)–(3),

$$\kappa_{\text{min}} = r^{1/\eta} \quad (4a)$$

$$\kappa_{\text{maj}} = (1-r)^{1/\eta}. \quad (4b)$$

Table I shows the values of r and η as obtained from experimental values of κ_{min} and κ_{maj} by solving Eq. (4).

We assume that when the flow through an airway falls below a critical threshold value Q_c , the gas transport transitions to diffusion and the airway is terminated by an air sac [4]. The cutoff diameter D_c at which airways terminate is given by $D_c = (Q_c)^{1/\eta}$.

From Eq. (1) we see that a daughter with an even (odd) index j inherits the diameter of the parent airway multiplied by a factor κ_{min} (κ_{maj}). The diameter $D_{i,j}$ can thus be expressed in terms of κ_{min} and κ_{maj} using the number of even and odd steps required to reach airway (i, j) from the root $(0, 0)$. At generation N , the diameters $D_{N,j}$ can take values $\kappa_{\text{maj}}^m \kappa_{\text{min}}^{N-m}$ where $m = 0 \dots N$ is the number of odd steps necessary to reach (N, j) from $(0, 0)$. Hence, we can express m as a function of the diameter D ,

$$m(D) = \frac{\log D - N \log \kappa_{\text{min}}}{\log \kappa_{\text{maj}} - \log \kappa_{\text{min}}}. \quad (5)$$

The number $\Omega_N(m)$ of airways at generation N corresponding to a particular m can be found by enumerating the number of ways one can select the m odd steps among the

TABLE I. Parameters for four species obtained from data [7,8] and used in the model. The mean \pm standard deviation of the diameter ratios κ_{maj} and κ_{min} are obtained from the data shown in Fig. 2. Also shown are the values of r and η obtained by solving Eq. (4).

Species	Data		Model	
	κ_{maj}	κ_{min}	r	η
Dog	0.927 ± 0.085	0.574 ± 0.117	0.198	2.92
Rat	0.865 ± 0.165	0.583 ± 0.182	0.286	2.32
Rabbit	0.887 ± 0.263	0.529 ± 0.203	0.237	2.26
Human	0.876 ± 0.097	0.686 ± 0.118	0.326	2.97

N steps, $\Omega_N(m) = \binom{N}{m}$. Using the Stirling formula,

$$\Omega_N(m) \approx 2^N \sqrt{\frac{2}{\pi N}} \exp\left[-\frac{(m - N/2)^2}{N/2}\right]. \quad (6)$$

Substituting m from Eq. (5) in Eq. (6), making a continuum approximation for m , and taking into account the cutoff at D_c , we obtain the distribution $\Pi_N(D)$ of diameters at generation N . Thus, $\Pi_N(D)dD \propto \Omega_N(m)dm\Theta(D - D_c)$, where $\Theta(x)$ is the Heaviside step function. After normalization, we obtain

$$\Pi_N(D) = \frac{A_N}{\Lambda_{N,1}} \exp\left[-\frac{\log^2(D/\kappa^N)}{2Ns^2}\right] \Theta(D - D_c). \quad (7)$$

The width and peak of the distribution $\Pi_N(D)$ are determined by $s \equiv \frac{1}{2} \log(\kappa_{\text{maj}}/\kappa_{\text{min}})$ and $\kappa \equiv \sqrt{\kappa_{\text{maj}}\kappa_{\text{min}}}e^{-s^2}$, respectively. The log-normal distribution is normalized by

$$A_N \equiv \sqrt{\frac{2}{\pi N s^2}} (\kappa e^{s^2/2})^{-N} \quad (8)$$

and $\Lambda_{N,1}$ reflects the effect of truncation at D_c , with

$$\Lambda_{N,q} = \text{erfc}\left[\left(\sqrt{\frac{N}{N_q}} - \sqrt{\frac{N_c}{N}}\right)\right], \quad (9)$$

where $N_c = \frac{1}{2s^2} \log^2 D_c$ and $N_q = 2s^2/(qs^2 + \log^2 \kappa)$. Figure 3 shows that $\Pi_N(D)$ predicted by Eq. (7) agrees well with empirical data on the dog lung.

The mean diameter $\langle D_N \rangle$ at generation N is given by

$$\langle D_N \rangle = (\kappa e^{3s^2/2})^N \frac{\Lambda_{N,2}}{\Lambda_{N,1}}. \quad (10)$$

For small N the effect of D_c is negligible, so the term $\Lambda_{N,2}/\Lambda_{N,1} \approx 1$ and the mean diameter decreases exponentially with N , $\langle D_N \rangle \approx (\kappa e^{3s^2/2})^N$. However, for large N , $\langle D_N \rangle$ approaches D_c . Figure 4(a) shows the calculated

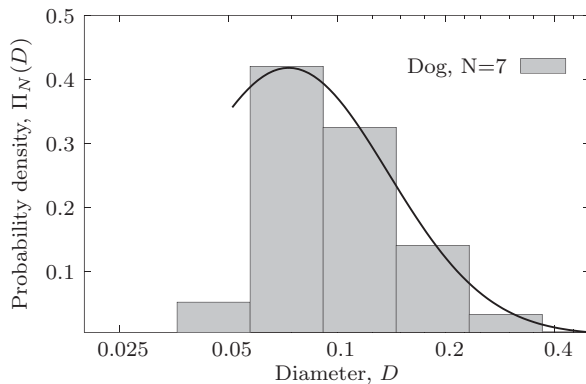


FIG. 3. Linear-log plot of a typical distribution $\Pi_N(D)$ of airway diameters D . Filled boxes show $\Pi_N(D)$ for a dog lung at generation $N = 7$. The solid line shows the model $\Pi_N(D)$ as given by Eq. (7) using the parameters in Table I.

$\langle D_N \rangle$ using the parameters in Table I in comparison to the measured data for four species.

In order to calculate the standard deviation $\sigma(D_N) \equiv [\langle D_N^2 \rangle - \langle D_N \rangle^2]^{1/2}$, we must calculate the second moment

$$\langle D_N^2 \rangle = (\kappa^2 e^{4s^2})^N \frac{\Lambda_{N,3}}{\Lambda_{N,1}}. \quad (11)$$

Figure 4(b) shows that $\sigma(D_N)$ calculated using our model compares well with the observed heterogeneity in measured data.

In order to investigate the functional consequence of the asymmetry [11], we next examine the resistance R of the airway tree. The Poiseuille flow resistance of an airway is given by $\rho_{i,j} \propto L_{i,j}(D_{i,j})^{-4}$, where $L_{i,j}$ is the length of airway (i, j) . We assume that $L_{i,j} \propto D_{i,j}$, i.e., the aspect ratios of the airways are conserved [4], so

$$\rho_{i,j} = \rho_{0,0}(D_{i,j})^{-3}, \quad (12)$$

where $\rho_{0,0}$ is the resistance of the trachea.

For a symmetric tree with $r = 1/2$, $\kappa = \kappa_{\text{maj}} = \kappa_{\text{min}} = 2^{-1/\eta}$ from Eq. (4), and thus the diameters $D_{i,j} = \kappa^i$ and

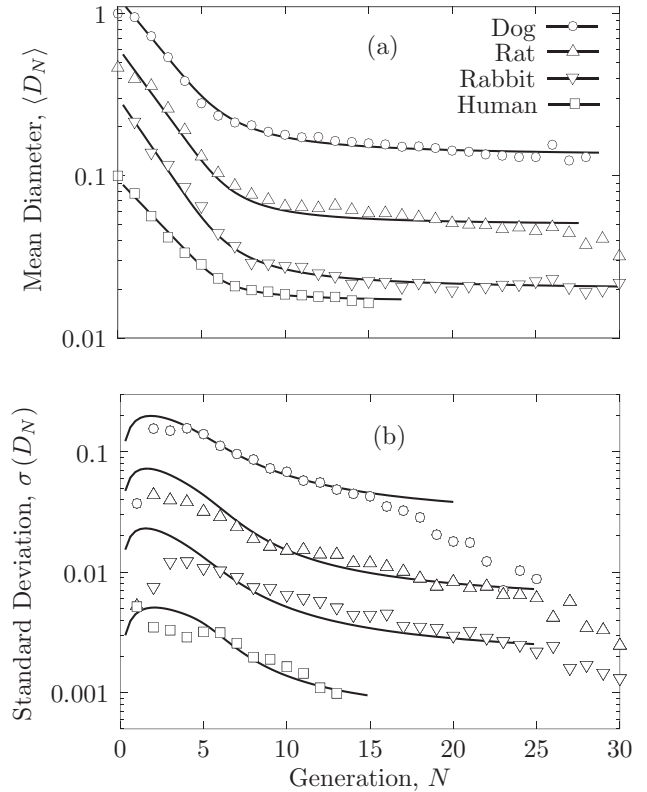


FIG. 4. Semilog plot of (a) mean diameters $\langle D_N \rangle$ and (b) standard deviation of the diameters $\sigma(D_N)$ plotted as a function of generation N for four species: dog (\circ), rat (\triangle), rabbit (∇), and human (\square). Solid lines show the model predictions using the parameters in Table I, and with $D_c = 0.084, 0.070, 0.053,$ and 0.165 , respectively, for the four species. The curves are vertically shifted for clarity.

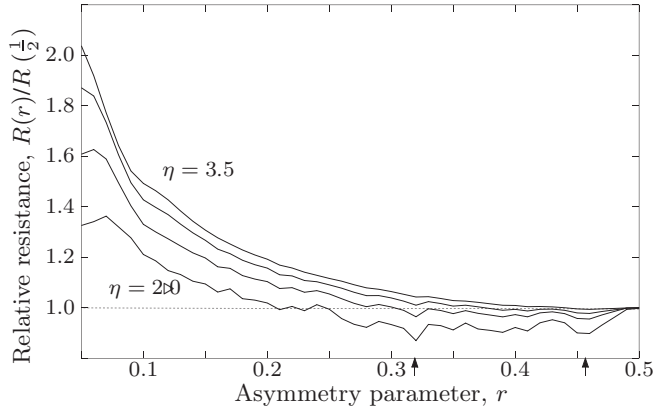


FIG. 5. Total resistance $R(r)$ of the airway tree relative to the resistance $R(\frac{1}{2})$ for a symmetric tree, as a function of r for $\eta = 2.0, 2.5, 3.0,$ and 3.5 , with $Q_c = 10^{-4}$. For certain values of r , indicated by arrows, the asymmetric tree has a lower R than the corresponding symmetric tree which is indicated by the dotted horizontal line.

the resistances $\rho_{i,j} = \rho_{0,0} w^i$ with $w = 2^{3/\eta}$ from Eq. (12). The total resistance R_M of a tree with M generations can be written using the recursion relation $R_M = \rho_{0,0} + (wR_{M-1} \parallel wR_{M-1})$, where $(a \parallel b) \equiv (a^{-1} + b^{-1})^{-1}$ is the equivalent resistance for a parallel combination. Thus,

$$R_M = \rho_{0,0} \sum_{i=0}^M \left(\frac{w}{2}\right)^i. \quad (13)$$

For $\eta > 3$ the series in Eq. (13) quickly converges to $R_M \approx \rho_{0,0}/(1 - \frac{w}{2})$ which is independent of the size of the tree, so most of the contribution to the resistance is from the airways with small i . However, for $\eta < 3$ the resistances of terminal airways ($i = M$) dominate R_M .

For a tree with $r < \frac{1}{2}$, asymmetry is introduced in two ways: (a) the two daughter subtrees of a bifurcating airway have different resistances since they have different diameters and (b) airways with smaller diameters reach the cutoff diameter D_c in fewer generations, resulting in missing subtrees. First we assume $D_c \rightarrow 0$ in order to eliminate the effect of the cutoff. The total resistance R_∞ of the resulting infinite tree can be written as

$$R_\infty = \rho_{0,0} + (w_{\min} R_\infty \parallel w_{\text{maj}} R_\infty), \quad (14)$$

where $w_{\min} = \kappa_{\min}^{-3}$ and $w_{\text{maj}} = \kappa_{\text{maj}}^{-3}$. The expression for R_∞ is analogous to the symmetric R given by Eq. (13) with $w/2 = (\kappa_{\min}^3 + \kappa_{\text{maj}}^3)^{-1}$, so R_∞ is finite when $\kappa_{\min}^3 + \kappa_{\text{maj}}^3 > 1$. Since $\kappa_{\min}^\eta + \kappa_{\text{maj}}^\eta = 1$ from Eq. (4) and $\kappa_{\min}, \kappa_{\text{maj}} \leq 1$, R_∞ converges for $\eta > 3$. Thus, for $\eta < 3$, terminal airways contribute significantly to the total tree

resistance and we cannot ignore the effect of the finite nature of the tree due to D_c .

To study the resistance R of a finite asymmetric tree, we used computer generated realizations for different values of r and η with fixed Q_c . Figure 5 shows the ratio of R for the asymmetric airway tree relative to R for a symmetric tree, for different η . For $\eta > 3$, the series in Eq. (13) converges, which is reflected by the monotonic decrease in R with increasing r . For $\eta < 3$ the curves are nonmonotonic functions of r as the terminal airways contribute significantly to R . We find local minima in R for certain values of r (arrows in Fig. 5).

We note that, while our assumption of Poiseuille flow is valid for smaller airways which are important for $\eta < 3$, turbulent and entrance effects are important for larger airways [12] which are the dominant contributors to R for $\eta > 3$. These effects are also responsible for the observed differences between inspiratory and expiratory R , which are identical in our model. Additionally, the elastic properties of the walls are not taken into account.

Finally, the nature of bifurcation asymmetry that determines the diameter distributions might be related to optimization of function within the constraints imposed by the shape of the lung. However, since the observed values of $\eta \lesssim 3$, our findings suggest that over a wide range of r , the asymmetry is not an appreciable impediment to the flow of air into gas exchange units of the lung.

This study was supported by NSF (BES-0402530) and Hungarian OTKA T42971.

-
- [1] *The Notebooks of Leonardo da Vinci*, edited by J.P. Richter (Dover Publications, New York, 1970).
 - [2] M. F. Shlesinger and B. J. West, Phys. Rev. Lett. **67**, 2106 (1991).
 - [3] K. Horsfield and A. Thurlbeck, Bull. Math. Biol. **43**, 681 (1981).
 - [4] H. Kitaoka and B. Suki, J. Appl. Physiol. **82**, 968 (1997).
 - [5] G. B. West *et al.*, Science **276**, 122 (1997).
 - [6] A. Majumdar *et al.*, Phys. Rev. E **67**, 031912 (2003).
 - [7] O. Raabe *et al.*, Tech. Rep. Publ. No. LF-53 (Lovelace Foundation for Medical Education and Research, Albuquerque, NM, 1976).
 - [8] R. Ramchandani *et al.*, J. Appl. Physiol. **90**, 1584 (2001).
 - [9] C. D. Murray, Proc. Natl. Acad. Sci. U.S.A. **12**, 207 (1926).
 - [10] H. B. Uylings, Bull. Math. Biol. **39**, 509 (1977).
 - [11] B. Mauroy *et al.*, Nature (London) **427**, 633 (2004).
 - [12] R. D. Ingram, Jr. and T. J. Pedley, in *Handbook of Physiology: The Respiratory System* (American Physiological Society, Bethesda, MD, 1986), pp. 277–293.